

Article

Study on the Evolution Pattern of the Aromatics of Lignin during Hydrothermal Carbonization

Wendi Sun ¹, Li Bai ^{2,*}, Mingshu Chi ^{1,*}, Xiuling Xu ³, Zhao Chen ¹ and Kecheng Yu ¹¹ School of Municipal and Environmental Engineering, Jilin Jianzhu University, Changchun 130118, China² Key Laboratory of Songliao Aquatic Environment Ministry of Education, Jilin Jianzhu University, Changchun 130118, China³ Library of Jilin Jianzhu University, Changchun 130118, China

* Correspondence: baili@jlju.edu.cn (L.B.); cms20062006@163.com (M.C.)

Abstract: Waste straw contains a large amount of lignin, and its resource utilization is not only in line with the national double carbon development strategy, but also to alleviate environmental pollution. Hydrothermal carbonization is a new thermochemical conversion technology, which has attracted much attention because it can directly transform carbon containing waste raw materials with high moisture content and low energy density. To investigate the physicochemical properties and aromatization changes of lignin hydrochar, hydrothermal carbonization experiments were carried out at 290 °C and a solid–liquid ratio of 1:20 for 0.00, 0.25, 0.50, 1.00, 1.50, 2.00, 4.00, 8.00 h, respectively. The experimental results shows that hydrothermal carbonization can increase the combustion quality of lignin. Physical and chemical properties analysis shows that with the increase of hydrothermal carbonization time from 0 to 2 h, the hydrochar content increased from 21.21% to 26.02% and the HHV of hydrochar increased from 20.01 MJ/Kg to 26.32 MJ/Kg. When the holding time exceeded 2 h, the carbon content and calorific value of hydrothermal tended to be stable. With the increase of holding time, FTIR analysis and XRD analysis show that the free hydroxyl groups in water-soluble lignin were easily combined with intramolecular and intermolecular hydrogen bonds, thus forming an ordered crystal arrangement. Subsequently, the crystal structure formed a well-arranged long chain through a strong hydrogen bond network, forming a ring structure in the process of aromatization. Aromatic ring structure accumulated, aromatization wave peak increased with holding time and aromatization intensified. Hydrochar crystal particles became larger and arranged in order. At the same time, the surface functional group detection and degree of crystallization were almost unchanged when holding time exceeded 2 h. The surface morphology of hydrochar was observed by SEM as follows: when the hydrothermal carbonization reaction of lignin entered the insulation stage, the microsphere structure began to aggregate and then became larger. When the holding time reached 2 h, the growth rate of carbon microspheres noticeably slowed. Therefore, the optimal hydrothermal carbonization time of lignin is 2 h, and hydrochar fuel has the best performance and aromatization.

Citation: Sun, W.; Bai, L.; Chi, M.; Xu, X.; Chen, Z.; Yu, K. Study on the Evolution Pattern of the Aromatics of Lignin during Hydrothermal Carbonization. *Energies* **2023**, *16*, 1089. <https://doi.org/10.3390/en16031089>

Academic Editor: Gabriele Di Giacomo

Received: 6 September 2022

Revised: 14 December 2022

Accepted: 24 December 2022

Published: 18 January 2023



Copyright: © 2023 by the authors. Licensee MDPI, Basel, Switzerland. This article is an open access article distributed under the terms and conditions of the Creative Commons Attribution (CC BY) license (<https://creativecommons.org/licenses/by/4.0/>).

Keywords: lignin; hydrothermal carbonization; holding time; fuel performance; aromaticity

1. Introduction

The exploitation and utilization of petroleum and other fossil resources in the long-term development of mankind not only causes a sharp reduction of fossil resources, but also brings huge environmental pollution problems. Lignin is one of the most abundant natural polymers with aromatic rings as structural units on earth has broad application fields and application prospects. The use of renewable lignin to replace petroleum and other fossil resources is of great significance to maintain carbon and oxygen balance in the biosphere and achieve sustainable development. The structure of lignin is very complex. It is a three-dimensional polymer compound composed of phenylpropane

structural units connected by carbon-carbon bond and ether bond. It contains a variety of active functional groups [1–5] and is an extremely complex network polymer randomly polymerized by carbon-carbon bond and ether bond between lignin monomers, without strict fixed structure. It is a complex polymer compound that exist in the xylem of most terrestrial plants, accounting for approximately 1/3 of the biomass of terrestrial plants. The content of lignin varies with plant types. The content of lignin in coniferous plants, broadleaf plants and herbaceous plants is 27–33%. As one of the main components of plants, 18–25% and 17–24% account for approximately 15–40% of the dry weight of lignocellulosic biomass, and lignin is high in carbon and oxygen content, with a mass fraction of approximately 60% and 30%, respectively. Lignin is the most abundant renewable organic resource with aromatic characteristics in nature [2,5–7]. In terms of total amount, the amount of lignin on earth is second only to cellulose. It is estimated that 150 billion tons of lignin can be produced by plant growth worldwide every year.

In fact, broadly speaking, lignin not only includes the kinds of lignin in plants, but the lignins that are present in different parts of cells with different morphology in various raw materials, and also includes the kind of unchanged lignin contained in plant tissue. These are known as “original lignin” (protolignin). The somewhat denatured lignin, which is extracted from plants with a neutral solvent, such as ethanol is called “natural lignin.” There is also Brauns lignin, named after Brauns, which is now believed to be part of the original lignin. Freudenberg calls it “soluble lignin” [6,8–14]. The term lignin now generally refers to the lignin products, which can be separated from plants as well as lignin derivatives.

Lignin has a wide range of sources, nor been well applied. Human have used cellulose for thousands of years, but lignin really only began to be studied after 1930, and has not been well used. The bulk of resources provided to humans by nature are wasted every year. The pulp and paper industry also provides a large source of lignin, which can reach more than 500 million tons of industrial lignin annually. However, these lignin resources have not been effectively used, and most of the pulp waste liquid is discharged or directly burned. Not only causes a serious waste of resources but also brings potential environmental problems.

As an environmentally friendly thermochemical conversion method, hydrothermal carbonization mainly generates solid product hydrochar through reactions, such as dehydration, condensation and decarboxylation of organic matter. Moreover, hydrothermal carbonization is a chemical method superior to combustion or pyrolysis of solid fuels. It has the advantages including no pre-drying treatment, high conversion efficiency, and relatively low operating temperature. It is easy to react with water-based biological waste, thereby avoiding the excessive consumption of energy for biomass waste drying treatment [3,4,12]. It has a great potential for development in the treatment of waste biomass.

Although it has been recognized that hydrothermal carbonization is the best solution for the commercial application of lignin, technical breakthroughs have not been made due to the lack of a comprehensive understanding of the structural evolution and aromatization reaction mechanism of lignin biomass [5,11,15]. According to previous studies, hydrolysis and aromatization are two important reactions of hydrothermal carbonization. Hydrolysis leads to the cracking of bonds in biological macromolecules, and aromatization leads to the formation of coal-like structures [5,11,15,16].

Studying the mechanism of lignin hydrothermal carbonization process has epoch-making significance for lignin resource utilization. However, hydrothermal carbonization process involves a lot of chemical reactions and molecular structure changes, so the generation of hydrothermal carbon, hydrothermal carbonization process reaction and structure changes were summarized, respectively.

The hydrothermal carbonization temperature of lignin is generally lower than 350 °C, and it is difficult to become water coke through aqueous solution homogeneous phase. Although some lignin can be dissolved in water at 200 °C, most lignin fragments

are difficult to dissolve and disperse into the aqueous phase [17]. Therefore, solid–solid transformation is preferred, and heterogeneous pyrolysis of non-soluble lignin produces polyaromatic hydrocarbon coke. Dissolved and undissolved lignin surface fragments exposed to water produce cracks and pores through hydrothermal carbonization. These fragments are decomposed into phenolic substances by hydrolysis and then polymerized into phenolic hydrochar. Some phenolic carbonates, especially those from surface fragments of insoluble lignin, are located on the surface of insoluble lignin or polyaromatic carbonates, and these cracks and pores are then filled or covered.

Reactions in the hydrothermal carbonization process include hydrolysis, dehydration, decarboxylation, aromatization, etc. [7,18]. Hydrothermal carbonization is a process in which macromolecules are degraded into small molecular fragments and reaggregated into macromolecules. It is a reaction between free groups. Due to the hydrothermal carbonation reaction in a closed environment and the complex structure of lignin, it is difficult to accurately describe the reaction path of lignin hydrothermal carbonation process, and some mechanisms are still unclear. However, the formation of products in the thermal decomposition process is closely related to the reaction mechanism of the regulatory process, and the hydrothermal carbonization of lignin uses water as the medium, so the hydrothermal carbonization of lignin starts from the hydrolysis reaction, but the hydrolysis is restricted by the mass transfer within the lignin, and the hydrolysis rate is determined by the diffusion progress. In the hydrolysis stage, the small molecular compounds are hydrolyzed into monomers, and the pH value of the system is reduced.

At the same time, dehydration occurred in the hydrothermal carbonization of lignin, which made the lignin remove water molecules. All kinds of soluble substances were formed after the reaction of carbon frame cracking and dehydration. Dehydration can still occur when the reaction process is low, but decarboxylation reaction is not obvious. Decarboxylation begins only after a large amount of water is generated. Decarboxylation is the elimination of part of the carboxyl group, and the rate of decarboxylation is usually much lower than that of dehydration.

Another source of water molecules in hydrothermal processes is condensation polymerization between fragments. Polycondensation can remove hydroxyl and carboxyl groups to form easily aggregated unsaturated substances, and then the intermolecular dehydration or aldol condensation to produce a large number of soluble polymers. Under hydrothermal conditions, these soluble polymers are highly reactive, and new polymers are generated through aromatization, which also leads to the formation of solid phase products in the hydrothermal process, which increases the aromatic structure of solid phase products and enhances the stability of hydrothermal carbon. At present, the literature on aromatization reaction is relatively few.

According to previous studies, hydrolysis and aromatization are two important reactions of hydrothermal carbonization. Hydrolysis leads to bond cracking in biological macromolecules, and aromatization converts hydrogenated aromatic compounds into aromatic compounds through dehydrogenation, leading to the formation of coal-like structures [19]. Aromatization of lignin in hydrothermal carbonization is a process in which aromatic hydrocarbon products are obtained from lignin solid residue through a series of reaction steps, such as hydrogen transfer, oligomerization and cyclic polymerization.

The aromatization reaction is complex and the influencing factors are extensive. In recent years, a large number of scholars at home and abroad have carried out some research work on this topic, such as exploring the influence of hydrothermal temperature, holding time and other reaction conditions on aromatization. The increase of hydrothermal carbonization reaction temperature increases the chemical stability and structural order of solid phase products [17], and thus improves the degree of aromatization of hydrothermal carbon. However, there are few studies on the influence of holding time on hydrothermal carbonization aromatization, which requires further study and discussion [6,13,20].

Aromatization refers to the reaction in which hydrogenated aromatic compounds are converted into aromatic compounds by dehydrogenation. During the reaction process, alkanes and olefins are cyclized and further hydrogen transfer reaction occurs. During the reaction process, hydrogen atoms are continuously released, and aromatization finally generates aromatic hydrocarbons. The aromatization reaction is a process in which the lignin solid phase residue undergoes a series of reaction steps, such as hydrogen transfer, oligomerization, and cyclization to obtain aromatic hydrocarbon products [8,11]. The reaction is a complex process, and there are many factors affect the aromatization reaction.

At present, hydrothermal carbonization is an important way to realize the efficient utilization of lignin. However, the evolution of lignin structure and aromatization mechanism during hydrothermal carbonization have not made significant progress so far. The aromatization process is complex and affected by temperature, holding time and other working conditions [14,21,22]. Increasing the temperature of hydrothermal carbonization will improve the aromatic degree, structural order and chemical stability of the product-hydrochar. However, there are few studies on the influence of holding time on the aromatization mechanism in hydrothermal carbonization and the chemical structure change of hydrothermal carbonization product-hydrochar. According to previous literature, other working conditions such as temperature can well increase the aromaticity and calorific value of hydrochar, nonetheless there is little research on the holding time [8,9,12,20]. On one basis, this paper discusses the influence of different holding time on aromaticity and calorific value, as well as the changes of physicochemical properties and aromatization mechanism of hydrochar, so as to provide theoretical basis for the research and development of efficient carbon aromatization system. This novel point is to explore the influence of the change of holding time on the aromatic degree and calorific value of hydrochar. The evolution process of chemical structure and physical form of hydrochar is discussed through ultra-fine time grouping, which provides mechanism research and theoretical support for realizing high-energy utilization of lignin. At the same time, the influence of hydrothermal carbonization reaction conditions on the chemical structure of hydrochar is a recent research hotspot. In this paper, by adjusting the holding time, the aromatization process of lignin during hydrothermal carbonization and the change rule of the aromatization degree of the product-hydrochar are studied by adjusting the holding time, and the change of the physicochemical properties and aromatization mechanism of hydrochar with the holding time were deeply explored, aiming to improve the theoretical support for the research and development of efficient utilization technology of lignin.

2. Materials and Methods

2.1. Materials

The lignin used in this study was purified from industrial paper mill waste liquid and the samples were dried directly at 105 °C for 24 h, followed by grinding, screening, and reprocessing for pre-drying. Samples of 400 g with a particle size <400 µm were selected and kept in a sealed bag for later use.

2.2. Experimental Device

The lignin hydrochar experiment was carried out in a 100 mL steel permanent magnet rotary mixing high-pressure reactor. The reactor consists of a heating furnace, reaction vessel, mixing device, transmission system and safety protection device. The main performance indexes were maximum working pressure 20 MPa, maximum working temperature 360 °C; heating power 0.8 KW, heating pressure regulating range 0–220 V, and mixing speed 0–300 r/min.

2.3. Experimental Protocol

The lignin hydrochar experiment was conducted at 290 °C and at a solid–liquid ratio of 1:20 for 0.00 h, 0.25 h, 0.50 h, 1.00 h, 1.50 h, 2.00 h, 4.00 h, and 8.00 h. The schematic diagram of hydrochar preparation by a hydrothermal reactor was shown in Figure 1. By analyzing the physicochemical properties and FTIR of hydrochar products, the effects of thermal insulation time on the physicochemical properties of hydrochar and the aromatization degree of hydrochar were studied.

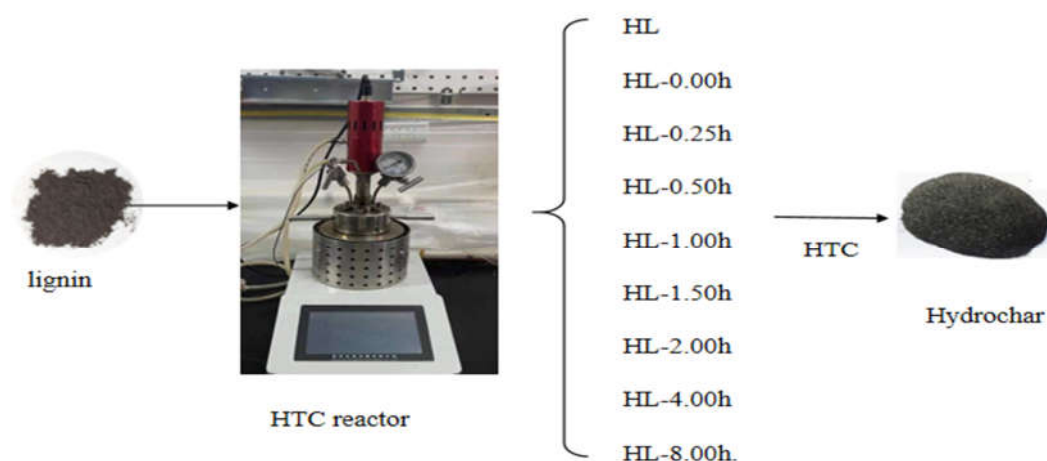


Figure 1. Schematic diagram showing the preparation of hydrochar.

A total of 3 g of lignin raw material were accurately weighed on the analytical balance and mixed with 60 mL of distilled water, creating a solid–liquid ratio of 1:20. Then, the mixture was placed in the reactor. After sealing the lid of the kettle, to ensure that the air in the kettle was completely eliminated, the speed of the magnetic mixer was set at 180 r/min. The kettle reaction temperature control is constant at 290 °C, and the heating rate was set at 5 °C/min. The reactor switch was turned on and the lignin hydrochar reaction experiment was conducted. Eight different experiments were conducted by controlling the holding times, repeating each group three times. After the hydrothermal reaction experiment, the reactor temperature drops rapidly. After reaching room temperature, the exhaust valve was opened to depressurize the reactor. Then, the kettle lid could be opened and the solid–liquid mixture was dumped into the filter device. Under the action of vacuum pump, the mixture was rinsed with distilled water several times until the filtrate was clear and the solid and liquid were separated.

The distillation was repeated and rinsed until the filtrate was clear at which point the solid and liquid separated. The hydrochar obtained from the experiment was dried in the oven (105 °C) to a constant mass, then ground, sieved with an 80-mesh sieve, and placed in a sealed bag for storage. The lignin raw materials and hydrochar generated under different thermal insulation conditions are numbered as HL, HL290-0, HL290-0.25, HL-0.50, HL-1.00, HL-1.50, HL-2.00, HL-4.00, and HL-8.00. The average value of three groups of parallel samples was used to calculate hydrochar yield (η_{yield} , %) and energy recovery efficiency (Renergy, %).

$$\eta_{\text{yield}} = (M_{\text{hydrochar}}/M_{\text{raw}}) \times 100\% \quad (1)$$

$$R_{\text{energy}} = (\text{HHV}_{\text{hydrochar}} \times \eta_{\text{yield}})/(\text{HHV}_{\text{raw}} \times \eta_{\text{yield}}) \times 100\% \quad (2)$$

(where $M_{\text{hydrochar}}$ is the mass of solid phase residue after hydrothermal heating (g); M_{raw} is the drying mass of raw materials added (g); $\text{HHV}_{\text{hydrochar}}$ is the calorific value of hydrothermal carbon (MJ/Kg); and HHV_{raw} (MJ/Kg) is the calorific value of raw materials).

2.4. Analysis Method

2.4.1. Industrial Analysis

The ash(A), volatile (VM), and carbon fixation (FC) content of the sample was determined by industrial analyzer (YX-GYFX 7706, Changsha Youxin Instrument Manufacturing Co., Ltd. (Changsha, China)). Specifically, the first two can be detected directly, and the latter is calculated by the difference method.

2.4.2. Elemental Analysis

The elemental analyzer (EA3000, Euro Vector, Milan, Italy) can be used to measure the C and H content in the sample. Take approximately 1 mg of the sample, wrap it in aluminum foil and form it into cylindrical pellets, and place it in the measuring instrument. After starting the instrument C, H, S, N and Ash content can be obtained after 2 h, and O content needs to be calculated based on the difference of air drying base.

2.4.3. Calorific Value Determination

The higher heating value (HHV) was measured with a bomb calorimeter (YX-ZR/Q 9704, Changsha Youxin Instrument Manufacturing Co., Ltd., Changsha, China) according to GB/T 213-2008. An automatic calorimeter is used to determine the calorific value of the sample. The 0.5 g sample is placed in the sealed oxygen bottle. Under the condition of sufficient oxygen, if the sample is fully burned, the heat released by the combustion is absorbed by the surrounding water, and the water temperature rises proportionally to the heat released by the sample combustion.

2.4.4. Crystal Structure Analysis

X-ray diffraction (XRD) is a favorable method for measuring the crystal structure of carbon materials, which can determine the structural parameters of carbon materials. XRD (DX-2700 XRD, Dandong Tongda Technology Co., Ltd. (Dandong, China)) measures amorphous carbon (C_a), aromatic degree (f_a), intercrystalline layer spacing (d_{002}), and grain size (L_a , L_c) [7,18,23,24]. This is used as a structural parameter to evaluate the accumulation structure of the carbon layer of a carbon material.

2.4.5. Analysis of Hydrochar Characteristics

The functional group structure of the sample was analyzed by Fourier transform infrared spectrometer (Frontier FTIR, USA). In total, 1 mg of the sample and 100 mg of KBr were ground and tableted together. These slices were scanned with a photometer in the range of 4000–400 cm^{-1} to determine the surface functional groups of the sample.

2.4.6. Surface Morphology Observation

The surface morphology and structure of the samples were observed by scanning electron microscope (FEI™ ESEM Quanta 450 FEG, USA). A scanning electron microscope (SEM) was used, approximately 5mg of the sample is evenly sprayed with gold to increase its conductivity. Then, it is enlarged by 5000 or 10,000 times according to the morphology and the needs of experimental analysis.

3. Results and Discussions

3.1. Physicochemical Properties of Lignin and Hydrochar

Industrial analyzers, elemental analyzers, automatic calorimeters and other measuring instruments were used to obtain the volatile matter (VM), ash (A), and fixed carbon (FC) contents, C, H, O element content, Heat value (HHV), Hydrochar yield (η), and energy recovery (R) with 9 samples. The basic property parameters of the hydrothermal carbon under different holding times are shown in Table 1.

Table 1. Chemical characteristics of lignin and hydrochar obtained at different holding times and energy recovery efficiency of hydrothermal process.

Sample	VM (%)	FC ^b (%)	A (%)	C (%)	H (%)	O ^a (%)	η (%)	HHV (MJ/kg)	R (%)
HL	62.82 ± 0.12	20.23 ± 0.43	18.65 ± 0.11	64.12 ± 0.34	4.45 ± 0.09	28.29 ± 0.78		17.98	
HL290-0.00	60.46 ± 0.17	22.21 ± 0.56	18.33 ± 0.31	64.57 ± 0.45	4.37 ± 0.13	28.34 ± 0.56	50.61 ± 1.35	20.01	40.32 ± 1.01
HL290-0.25	60.33 ± 0.22	23.26 ± 0.37	17.41 ± 0.25	65.41 ± 0.37	4.26 ± 0.17	28.40 ± 0.39	51.22 ± 1.22	20.76	40.41 ± 1.23
HL290-0.50	57.74 ± 0.31	25.12 ± 0.41	17.14 ± 0.37	65.95 ± 0.28	4.21 ± 0.45	29.56 ± 0.66	52.43 ± 1.27	21.89	40.47 ± 1.45
HL290-1.00	55.21 ± 0.16	27.37 ± 0.38	16.42 ± 0.11	66.80 ± 0.39	3.77 ± 0.37	29.68 ± 0.49	53.64 ± 1.31	21.01	40.55 ± 1.66
HL290-1.50	53.24 ± 0.15	31.11 ± 0.57	15.65 ± 0.45	67.62 ± 0.47	3.68 ± 0.56	29.78 ± 0.37	54.18 ± 0.43	24.53	40.62 ± 1.24
HL290-2.00	52.13 ± 0.32	32.02 ± 0.39	14.85 ± 0.67	67.68 ± 0.39	3.07 ± 0.78	29.88 ± 0.29	55.31 ± 1.27	26.32	40.71 ± 1.42
HL290-4.00	52.08 ± 0.24	32.34 ± 0.51	14.58 ± 0.48	67.88 ± 0.29	3.04 ± 0.89	29.95 ± 0.38	55.35 ± 0.68	26.33	40.73 ± 1.31
HL290-8.00	52.03 ± 0.45	32.81 ± 0.62	14.16 ± 0.56	67.92 ± 0.47	3.01 ± 0.49	29.99 ± 0.18	55.37 ± 1.56	26.35	40.74 ± 1.52

^a By difference: O% = 100% – C% – H%, ^b By difference: FC% = 100% – VM% – A%.

By analyzing the data in Table 1, it can be concluded that:

(1) With the increase of holding time (0–2 h), volatile matter (VM) content decreased from 60.46% (0 h) to 52.13% (2 h), and fixed carbon (FC) content increased from 21.21% (0 h) to 32.02% (2 h). For example, when holding time was 1h, hydrochar VM decreased by 7.61% and FC increased by 2.68% compared with lignin raw material, which was consistent with the analysis in the literature that soluble intermediates form FC simultaneously on the surface of water coke through aromatization, thus increasing the proportion of FC in hydrochar. C content (0 h) rose to 64.57% from 67.68% (2 h), H content (0 h) reduced by 4.37% to 3.07% (2 h), O content (0 h) rose to 28.34% from 29.88% (2 h). When the holding time exceeded 2 h, the content of volatile fixed carbon changed slowly.

(2) The calorific value (HHV) varied with the content of volatile carbon (VM) and fixed carbon (FC) in hydrochar changes when the holding time increased (0–2 h). The calorific value of hydrochar increased from 20.01 MJ/Kg (0 h) to 26.32 MJ/Kg (2 h). When the holding time exceeded 2h, the calorific value of hydrochar did not change significantly and tended to be flat. Overall, the hydrochar yield (η) increased with the holding time, leading to an increasing trend of energy recovery efficiency (R) with the holding time, but not significantly [12,19]. This phenomenon could be explained by the increase of hydrochar content and the decrease of oxygen and hydrogen content in Table 1.

(3) With the increase of holding time (0–2 h), the proportion of C showed a steady upward trend (consistent with the increase of FC), while the proportion of oxygen and hydrogen decreased rapidly. The fluctuation of elemental content of hydrochar indicated the change of its chemical structure, and dehydration might occur during hydrothermal carbonization. The decarboxylation reaction released hydrogen and oxygen in the form of H₂O and CO₂, respectively. With increasing carbon content, the hydrothermal carbonization aromatization reaction intensified. After the holding time exceeded 2 h, the content of hydrochar changed slowly and the aromatization process basically ended.

In conclusion, hydrothermal carbonization could increase the combustion quality of lignin, the heat value of hydrothermal carbonization product-hydrochar increased from 0 to 2 h, from 20.01 MJ/Kg to 26.32 MJ/Kg. At the same time, the fixed carbon content in hydrochar increased from 21.21% to 26.02%, and the corresponding volatile content decreased from 60.46% to 52.13%. The calorific value of carbon content in hydrochar tended to change gently after holding time exceeded 2 h. From the perspective of fuel utilization, the optimal holding time was 2 h. With the increase of holding time (0–2 h), the proportion of C showed a stable upward trend (consistent with the increase of FC), while the proportion of oxygen and hydrogen decreased rapidly in which the proportion of O decreased from 28.34% to 23.21%, and the proportion of hydrogen decreased from 4.37% to 3.07%. The results showed that with the increase of holding time, the aromatization process of hydrothermal carbonization was accelerated and the aromatization degree

was increased. After holding for more than two hours, the aromatic degree of hydrothermal carbon did not change significantly.

3.2. Evolution of the Surface Functional Groups

After the hydrothermal carbonization of lignin, its surface functional group distribution changes.[18,25,26]. The infrared map of lignin and hydrochar with different insulation times was obtained by FTIR in Figure 2.

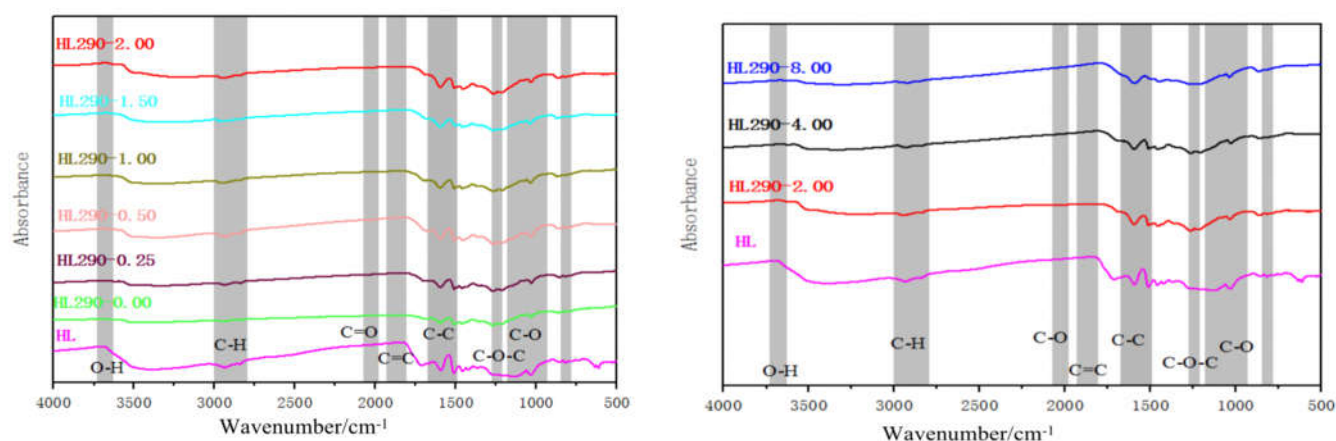


Figure 2. Infrared spectra of lignin and its hydrothermal carbon at different holding times.

Analysis of Figure 2 shows that:

(1) C-O stretching vibration peak at 1250–1000 cm^{-1} corresponds to the C-O peak of lignin and hydrochar, indicating the existence of oxygen-containing functional groups. Therefore, lignin and hydrochar have adsorption properties. The stretching vibration of hydroxyl (-OH) corresponding to the absorption peak near 3500–3000 cm^{-1} shows that the peak strength of hydrochar hydroxyl (-OH) is weaker than that of lignin raw material, and the peak strength of hydrochar hydroxyl (-OH) is further weakened with the increase of holding time [7,25,27–30]. The main reason is that the dehydration reaction of materials in the hydrothermal process, with the increase of the insulation time, the degree of dehydration reaction is gradually intensified. At 3100–2800 cm^{-1} , the stretching vibration peak of aliphatic group (-CH₂) is stronger than that of lignin, indicating that there are enriched hydrocarbons in the hydrochar. The vibration spectrum peak at 1700 cm^{-1} (C=O) was strengthened or appeared, indicating that decarboxylation reaction took place, and the C=O bond was formed by dehydration of hydroxyl groups, which may form carbonyl or carboxyl groups. With the increase of holding time, the peak intensity decreased, indicating that the reaction intensity increased as the mono-aromatic compounds were transformed into polyaromatic compounds. A stretching vibration peak appeared at 1600 cm^{-1} (C=C), indicating that aromatic rings were present in the sample and aromatization occurred during hydrothermal process. At the same time, with the increase of hydrothermal holding time, the spectral peak is strengthened and the aromatization degree is deepened.

(2) At the beginning of heat preservation, the vibration peak of -OH and CH₂ began to disappear, indicating that obvious pyrolysis reaction of lignin took place at this time. At the same time, C=O vibration peak appeared near 1700 cm^{-1} , indicating the formation of the intermediate product, L-glucosone.

(3) With the increase of holding time (0–2 h), the vibration peak of C=O weakens and the vibration peak of C=C increases, indicating that with the increase of holding time, the carbonyl group is removed in the form of CO and CO₂, and the resulting free carbon atoms undergo intramolecular and intermolecular bonding and rearrangement to form carbon six-membered ring and subsequent dehydrogenation to generate aromatic ring structure[26,30]. Meanwhile, the C-H bond of the aromatic ring structure near 870

cm^{-1} is strengthened, while the absorption peaks near 800 cm^{-1} and 750 cm^{-1} are weakened, indicating that the substitution sites in the aromatic ring are increasing, more ring structures were formed, and the carbon net plane, which forms the basic unit of the carbon microcrystalline is expanding [31]. This analysis conclusion is consistent with that of Table 1. According to the analysis of elemental content changes in physicochemical properties in Table 1, it is believed that aromatization may have occurred and the increase of holding time resulted in the increase of carbon content and intensification of aromatization. From the perspective of functional group change, FTIR analysis confirmed that aromatization intensified with the increase of holding time.

(4) When the thermal holding time is over 2 h, the $\text{C}=\text{C}$ bond is enriched gently. The peak positions of these spectra lines are basically the same, but there are slight differences in peak intensity. Due to the aromatization of lignin has been basically completed, the increase of the thermal insulation time has no significant impact [7,28,29,32].

It was found by FTIR that $-\text{C}-\text{H}-$, $-\text{C}=\text{C}$, and $-\text{C}-\text{O}$ bonds related to aromatic structure were gradually formed during hydrothermal process. Studies on the changes of surface functional groups shows that lignin, as a phenolic polymer, undergoes cleavage and condensation reactions during degradation, in which $-\text{C}-\text{O}-\text{C}$ is cleaved and oligomeric residues are generated [31,32]. Then, the intermediates are hydrolyzed to produce oxygen-containing hydrocarbons with 2–6 carbon atoms and substituted phenols, which accumulated in the reaction medium and resulted in the formation of aromatic $\text{C}-\text{C}$ and $-\text{C}=\text{C}$ by a large number of hydroxyl radicals. Subsequently, phenolic carbonates are synthesized by aromatization and polymerization. The structural changes of lignin during hydrothermal carbonization show that aromatization is the key mechanism of hydrothermal carbonization. FTIR analysis shows that with the increase of holding time, the enrichment of hydrocarbon $\text{C}=\text{C}$ bond in hydrochar increases significantly, the aromatization process intensifies, and the aromatic degree of hydrochar increases.

3.3. Crystal Structure Changes (XRD Analysis)

X-ray diffraction (XRD) non-destructive testing method is used to determine the crystal structure of lignin and hydrochar at different holding times in the experiment, as shown in Figure 3. From the changes of hydroxyl functional groups in Figure 3, it is inferred that free hydroxyl groups in water-soluble lignin can easily combine with intramolecular and intermolecular hydrogen bonds, thus forming an ordered crystal arrangement [26]. Subsequently, the crystal structure forms a well-arranged long chain through a strong hydrogen bond network, forming a ring structure in the process of aromatization [30]. This is consistent with the yield of hydrochar increasing with the increase of holding time (Table 1), and the analysis results of functional groups of hydrochar change with holding time (Figure 2). At the same time, the degree of crystallization is almost unchanged when holding time exceeds 2 h, the degree of crystallinity is the highest when holding time is 2 h.

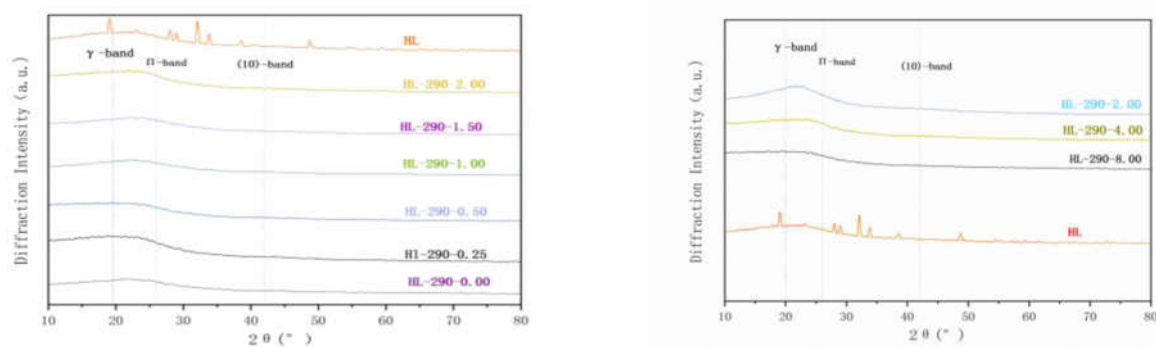


Figure 3. X-ray spectra of lignin and its hydrothermal carbon at different holding times.

The diffraction patterns were then deconvoluted with Origin software. The wide peaks in the 0–45° region can be fitted into three Gaussian peaks near 20 (γ-band), 26 (π-band), and 42 (10 band) [26,30–34]. The γ-band represents aliphatic carbon (Cal), and the π-band represents aromatic carbon (Car). According to the processed diffraction pattern, some structural parameters can be calculated, such as the layer spacing of the aromatic degree (fa), crystal structure, and the grain size (La, Lc) [33,34], which are summarized in Table 2.

In Table 2, aromaticity represents the proportion of aromatic carbon in the structure of water coke. $A\pi$ and $A\gamma$ are equal to the area aromaticity of the π-band and γ-band, respectively, as shown in Formula (3).

$$fa = Car/(Car + Cal) = A\pi/(A\pi + A\gamma) \quad (3)$$

($A\pi$ and $A\gamma$ is equal to the area of π band and γ band respectively).

The maturity of hydrochar (coal level) is calculated by the ratio of π-band intensity and γ-band intensity, and the wave intensity is denoted by I. The coal level formula is shown in Formula (4).

$$\text{Coal rank} = I\pi/I\gamma \quad (4)$$

Crystal structures, such as lateral size (La) and stacking height (LC), are also calculated by the traditional Scherrer equation as (5) and (6), respectively.

$$La = 1.84\lambda/B\cos(\varphi_a) \quad (5)$$

$$Lc = 0.89\lambda/B\cos(\varphi_c) \quad (6)$$

where λ is the radiation wavelength of Cu K α , Ba and Bc represent the maximum width of peak values of 10°-band and π-band, respectively. φ_a and φ_c are the number of carbon layers (N) in the structure of water coke. The formula is (7).

$$N = Lc/d002 \quad (7)$$

Combined with the analysis in Figure 3 and Table 2, it is found that the π-band gradually becomes narrower with the increase of holding time (related to the decrease of La), indicating that the disordered crystal gradually transforms into a transitional crystal (an intermediate structure between crystalline and amorphous states) [7,18,35]. In the hydrothermal process, the graphene sheets accumulate stably (consistent with the increase of Lc), the number of carbon layers is increased by disordered arrangement, and it almost completely transforms into ordered crystal, at 2 h. Baysal et al. [35] and Sonilbare et al. [34] believe that the increase of holding time might be an important factor for the increase of hydrochar aroma. The above study confirms this conclusion. With the increase of holding time, the coal grade ($I\pi/I\gamma$) of hydrochar is improved [31,32,34]. The higher the crystallinity of the hydrochar, the stronger is the aromatization.

The parameters of amorphous carbon (Ca) aromatics (fa) intergranular spacing (d002) and grain size (La, Lc) were measured by XRD to the structural change of carbon layer stacking structure shows that with the increase of holding time (0–2 h), the π-band gradually widens, and the γ- and π-band also merge into a wide peak (related to the increase of La). At this time, the disordered crystal gradually changes to transition crystal (an intermediate structure between crystalline and amorphous states), and the crystallinity of hydrochar is ordered and the crystal becomes larger. With the increase of holding time, the aromatization process of hydrothermal carbonization is intensified, and the ordered crystallinity of hydrothermal carbonization is enhanced, the thermal stability is enhanced, and the aromatization becomes higher. The maximum crystallinity aromaticity occurs at 2 h holding time.

Table 2. Structural parameters of lignin and thermal materials for different insulation times.

Sample	Peak are/%		Structure Parameters				
	γ -Band	π -Band	La/nm	Lc/nm	N	$I\pi/I\gamma$	Aromaticity
HL	11.32	12.21	3.56	0.85	2.14	1.11	0.54
HL290-0.00	12.33	12.54	3.66	0.82	2.12	1.14	0.52
HL290-0.25	12.35	12.64	3.78	0.81	2.15	1.15	0.51
HL290-0.50	12.38	12.75	3.79	0.82	2.16	1.19	0.53
HL290-1.00	12.41	12.87	3.75	0.73	2.17	1.22	0.52
HL290-1.50	12.42	13.88	3.86	0.74	2.17	1.23	0.51
HL290-2.00	12.45	13.76	3.64	0.72	2.18	1.24	0.54
HL290-4.00	12.51	14.79	3.56	0.71	2.19	1.24	0.53
HL290-8.00	12.67	14.80	3.45	0.81	2.34	1.25	0.55

3.4. Surface Topography of Lignin and Hydrochar

SEM was used to analyze the surface morphology of lignin and hydrochar at different holding times. The following 4 groups of SEM images were observed, as shown in Figure 4. According to the observation and analysis of Figure 4, it can be concluded that:

(1) Increasing the holding time can make the pore structure of hydrochar loose and improve the combustion performance. Lignin is composed of smooth spherical particles with a very small diameter. Many small irregular bright spots are attached on the surface of the particles, which is its broken crystal structure. The hydrochar in Figure 4a–d showed irregular porous honeycomb carbon block under scanning electron microscope. With the increase of holding time, the size of hydrochar particles tends to be uniform and agglomerate; and the diameter also increases to nanometer level, and the structure becomes loose. The surface of the hydrochar generated by hydrothermal carbonization has a certain pore structure, which makes it easier for the air flow to penetrate the interior of the particles during the combustion process of the hydrochar, conducive to complete combustion [30–32]. Increasing the holding time makes the pore structure more loose and the combustion more complete, consistent with Table 1, combustion performance increases with the increase of holding time. As seen in Table 2, interlayer spacing and grain size variation of crystal structure explain the reason for the change of pore structure and morphology of hydrochar, that is, with the increase of holding time, the aromatic degree increases, grain size increases, layer spacing increases, and the pore structure becomes loose. It is concluded that the increase of holding time intensifies the aromatization in hydrothermal carbonization and enhances the performance of the fuel with developed pore structure and calorific value.

(2) The optimal hydrothermal carbonization holding time is 2 h. The SEM images obtained by analysis (Figure 4) showed the following rules: When the holding time was 0 h, as shown in Figure 4a, small microspheres were initially formed on the surface of the hydrochar with uneven distribution, and pore structures were clearly visible on the surface. When the holding time is 1.00 h, as shown in Figure 4b, the hydrochar particles gradually become larger with the holding time increasing, and the surface becomes coarser, the structure is convex and even forms strips. As shown in Figure 4c, when the holding time reaches 2.0 h, the morphology of hydrochar microspheres presents uneven agglomerated particles, and the surface of the hydrochar microspheres presents a change of multi-layer structure with developed pore structure. Meanwhile, the dispersion of hydrochar microspheres is relatively uniform, and the particle size increases significantly to the nanometer level. As shown in Figure 4d, the structure of microspheres did not change significantly with the increase of holding time. Therefore, the aromaticity of hydrochar increased with the increase of holding time, reached a peak at 2 h and did not increase significantly after 2 h. This indicates that the optimal insulation time is 2 h.

(3) The SEM images show that the surface of hydrochar generated by hydrothermal carbonization has a certain pore structure. With the increase of holding time (0–2 h),

uneven and small microsphere structures were formed on the surface of hydrochar. It gradually evolved into a strip structure with a large agglomeration of particles, and its surface gradually changed into a uniform microsphere with a multi-layer structure. It can be inferred that the aromatization progress accelerates with the increase of holding time and the change is not obvious after 2 h. From the perspective of energy saving, the best insulation time is 2 h.

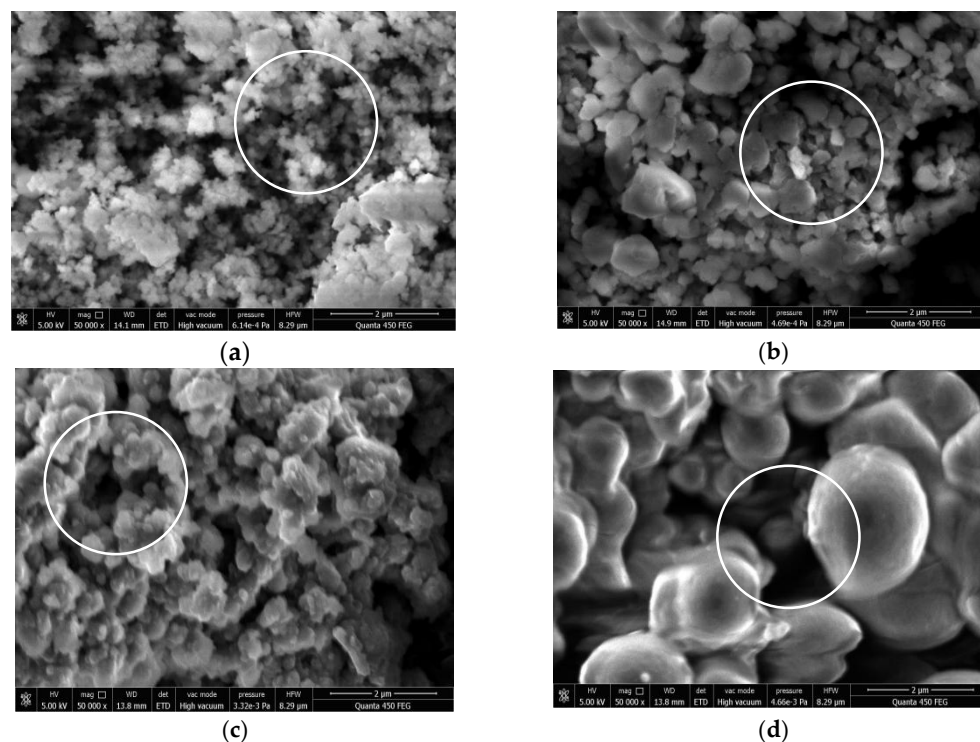


Figure 4. Scanning electron microscope images of lignin and hydrothermal charcoal at magnification 5000 at different holding times ((a): HL290-0.00, (b): HL-290-1.00, (c): HL-290-2.00, (d): HL-290-8.00).

4. Conclusions

In this paper, lignin was used as raw material to explore the effect of holding time on the combustion performance and aroma degree of hydrothermal carbonated aromatization products. Based on the study of the effect of holding time on the physicochemical properties of hydrothermal carbonization process, the influence of the combustion performance of hydrochar with holding time was investigated by means of industrial element analysis and other physicochemical measurement methods. FTIR, XRD, and SEM analysis methods were used to study the influencing factors of aromatization and aromatic degree change in the hydrothermal carbonization process and the high utilization potential of hydrothermal carbonization product hydrochar was evaluated.

The main conclusions are: with the increase of holding time, the fuel performance of hydrochar is enhanced and then the calorific value of hydrochar is increased. The heat value of hydrochar increases from 0 to 2 h, and the heat value of hydrochar increases from 20.01 MJ/Kg to 26.32 MJ/Kg. With the increase of time, the aromatization intensifies and the -C-H-, -C=C, and -C-O bonds related to aromatic structure are gradually increased during the hydrothermal process, which makes the aromatic degree of hydrochar become larger. With the increase of holding time (related to the decrease of L_a), π -band gradually becomes narrower, indicating that the disordered crystal gradually transforms into a transitional crystal (an intermediate structure between crystalline and amorphous states). The morphology and structure of hydrochar become orderly, the crystallinity and thermal stability are enhanced. The optimal thermal carbonization time of lignin is 2 h,

and the performance of hydrochar fuel is the best, and the aroma reached the peak. The relationship between the fuel properties and aromatization of hydrochar was explained, and the influence mechanism of holding time on the properties and aromatization of hydrothermal carbonized lignin fuel was explored, which provided a perfect theoretical basis for energy utilization of waste lignin.

Author Contributions: Conceptualization, M.C. and X.X.; methodology, W.S. and L.B.; validation, L.B. and M.C.; investigation, W.S., Z.C. and K.Y.; data curation, W.S. and M.C.; writing—original draft preparation, W.S.; writing—review and editing, L.B.; funding acquisition, L.B. and M.C. All authors have read and agreed to the published version of the manuscript.

Funding: This work was supported by the National Natural Science Foundation of China (52070088), National Natural Science Foundation of China (52100146), Jilin Science and Technology Bureau Outstanding Young Talents Training Special Project (No. 20200104118), Scientific Research Project of Education Department of Jilin Province (No. JJKH20210263KJ) and the Ministry of Housing and Urban-rural Development of China (2021-K-118). The research collaboration among the groups and universities of the authors is also appreciated.

Institutional Review Board Statement: Not applicable.

Informed Consent Statement: Not applicable.

Data Availability Statement: Data is contained within the article.

Conflicts of Interest: The authors declare no conflict of interest.

References

- Gadhave, R.V.; Mahanwar, P.A.; Gadekar, P.T. Lignin-polyurethane based biodegradable foam. *Open J. Polym. Chem.* **2018**, *8*, 1–10.
- Im, S.H.; Kim, G.; Oh, H.S.; Jo, S.; Kim, D. Hierarchy Decoder is All You Need To Text Classification. *arXiv* **2021**, arXiv:2111.11104.
- Porto, D.D.S.; Estevão, B.M.; Pincela Lins, P.M.; Rissi, N.C.; Zucolotto, V.; da Silva, M.F.G. Orange Trunk Waste-Based Lignin Nanoparticles Encapsulating Curcumin as a Photodynamic Therapy Agent against Liver Cancer. *ACS Appl. Polym. Mater.* **2021**, *3*, 5061–5072.
- Cao, L.; Iris, K.M.; Liu, Y.; Ruan, X.; Tsang, D.C.; Hunt, A.J.; Ok, Y.S.; Song, H.; Zhang, S. Lignin valorization for the production of renewable chemicals: State-of-the-art review and future prospects. *Bioresour. Technol.* **2018**, *269*, 465–475.
- Ming, H.; Jwhk, B.; Cheng, H.; Lim, S.H.H.; Cho, J.; Lateef, A.; Mak, A.; Tay, S.H. A meta-analysis of clinical manifestations in asian systemic lupus erythematosus: The effects of ancestry, ethnicity and gender. *Semin. Arthritis Rheum.* **2021**, *52*, 151932.
- Zhang, X. Research on the Preparation of Multifunctional Biochar by Hydrothermal Carbonization of Typical Waste Biomass. Thesis, Dalian University of Technology, Dalian, China, 2019.
- Heidari, M. Challenges and Opportunities of Hydrothermal Carbonization of Biomass. PhD Thesis. University of Guelph, Guelph, ON, USA, 2020.
- Gallant, R.; Farooque, A.A.; He, S.; Kang, K.; Hu, Y. A Mini-Review: Biowaste-Derived Fuel Pellet by Hydrothermal Carbonization Followed by Pelletizing. *Sustainability* **2022**, *14*, 12530.
- Zhao, J.; Sun, M.; Zhang, L.; Hu, C.; Tang, D.; Yang, L.; Song, Y. Forced Convection Heat Transfer in Porous Structure: Effect of Morphology on Pressure Drop and Heat Transfer Coefficient. *J. Therm. Sci.* **2021**, *30*, 363–393.
- Gillet, S.; Petitjean, L.; Aguedo, M.; Lam, C.H.; Blecker, C.; Anastas, P.T. Impact of lignin structure on oil production via hydroprocessing with a copper-doped porous metal oxide catalyst. *Bioresour. Technol.* **2017**, *233*, 216–226.
- Senel, K.; Bjrnson, E.; Larsson, E.G. Human and Machine Type Communications can Coexist in Uplink Massive MIMO Systems. In Proceedings of the 2018 IEEE International Conference on Acoustics, Speech and Signal Processing (ICASSP), Calgary, AB, Canada, 15–20 April 2018.
- Seyedsadr, S.; Al Afif, R.; Pfeifer, C. Hydrothermal carbonization of agricultural residues: A case study of the farm residues-based biogas plants. *Carbon Resour. Convers.* **2018**, *1*, 81–85.
- Scrinzi, D.; Ferrentino, R.; Baù, E.; Fiori, L.; Andreottola, G. Sewage Sludge Management at District Level: Reduction and Nutrients Recovery via Hydrothermal Carbonization. *Waste Biomass Valorization* **2022**, *2022*, 1–13.
- Sharma, H.B.; Sarmah, A.K.; Dubey, B. Hydrothermal carbonization of renewable waste biomass for solid biofuel production: A discussion on process mechanism, the influence of process parameters, environmental performance and fuel properties of hydrochar. *Renew. Sustain. Energy Rev.* **2020**, *123*, 109761.
- Mau, V.; Gross, A. Energy conversion and gas emissions from production and combustion of poultry-litter-derived hydrochar and biochar. *Appl. Energy* **2018**, *213*, 510–519.

16. Ermeko, T.; Mohammed, A.Y.; Wodera, A.L. Acceptability of PIHTC among TB Patients in Bale Robe Hospital, Southeast Ethiopia. *Int. J. Public Health Saf.* **2021**, *6*, <https://doi.org/10.37421/2736-6189.2021.6.217>.
17. Zhuang, X.Z.; Zhan, H.; Huang, Y.Q.; Song, Y.P.; Yin, X.L.; Wu, C.Z. Denitrification and desulphurization of industrial bio-wastes via hydrothermal modification. *Bioresour. Technol.* **2018**, *254*, 121–129.
18. Baysal, M.; Yurum, A.; Yildiz, B.; Yurum, Y. Structure of some western Anatolia coals investigated by FTIR, Raman, C^{13} solid state NMR spectroscopy and X-ray diffraction. *Int. J. Coal Geol.* **2016**, *163*, 166–176.
19. Xue, Y.; Bai, L.; Chi, M.; Xu, X.; Tai, L.; Chen, Z.; Yu, K.; Liu, Z. Co-hydrothermal carbonization of lignocellulose biomass and polyvinyl chloride: The migration and transformation of chlorine. *Chem. Eng. J.* **2022**, *446*, 137155. <https://doi.org/10.1016/j.cej.2022.137155>.
20. Zhuang, X.Z.; Huang, Y.Q.; Song, Y.P.; Zhan, H.; Yin, X.L.; Wu, C.Z. The transformation pathways of nitrogen in sewage sludge during hydrothermal treatment. *Bioresour. Technol.* **2017**, *245*, 463–470.
21. Gao, W.; Zhang, M.; Wu, H. Bed agglomeration during bio-oil fast pyrolysis in a fluidized-bed reactor. *Energy Fuel* **2018**, *32*, 3608–3613.
22. Shu, R.; Xu, Y.; Ma, L.; Zhang, Q.; Wang, C.; Chen, Y. Controllable production of guaiacols and phenols from lignin depolymerization using Pd/C catalyst cooperated with metal chloride. *Chem. Eng. J.* **2018**, *338*, 457–464.
23. Popescu, M.C.; Froidevaux, J.; Navi, P.; Popescu, C.M. Structural modifications of *Tilia cordata* wood during heat treatment investigate by FT-IR and 2D IR correlation spectroscopy. *J. Mol. Struct.* **2013**, *1033*, 176–186.
24. Smith, A.M.; Singh, S.; Ross, A.B. Fate of inorganic material during hydrothermal carbonisation of biomass: Influence of feed-stock on combustion behaviour of hydrochar. *Fuel* **2016**, *169*, 135–145.
25. Xue, Y.; Bai, L.; Chi, M.; Xu, X.; Chen, Z.; Yu, K.; Liu, Z. Co-hydrothermal carbonization of pretreatment lignocellulose biomass and polyvinyl chloride for clean solid fuel production: Hydrochar properties and its formation mechanism. *J. Environ. Chem. Eng.* **2022**, *10*, 106975.
26. Xin, S.Z.; Yang, H.P.; Chen, Y.Q.; Yang, M.F.; Chen, L.; Wang, X.H.; Chen, H. Chemical structure evolution of char during the pyrolysis of cellulose. *J. Anal. Appl. Pyrolysis* **2015**, *116*, 263–271.
27. He, C.; Zhao, J.; Yang, Y.; Wang, J.Y. Multiscale characteristics dynamics of hydrochar from hydrothermal conversion of sewage sludge under sub- and near-critical water. *Bioresour. Technol.* **2016**, *211*, 486–493.
28. Keiluweit, M.; Nico, P.S.; Johnson, M.G.; Kleber, M. Dynamic molecular structure of plant biomass-derived black carbon (biochar). *Environ. Sci. Technol.* **2010**, *44*, 1247–1253.
29. Liu, D.W.; Yu, Y.; Wu, H.W. Differences in water-soluble intermediates from slow pyrolysis of amorphous and crystalline cellulose. *Energy Fuels* **2013**, *27*, 1371–1380.
30. Fu, P.; Hu, S.; Sun, L.S.; Xiang, J.; Yang, T.; Zhang, A.; Zhang, J. Structural evolution of maize stalk/char particles during pyrolysis. *Bioresour. Technol.* **2009**, *100*, 4877–4883.
31. Harvey, O.R.; Herbert, B.E.; Kuo, L.J.; Louchouart, P. Generalized two-dimensional perturbation correlation infrared spectroscopy reveals mechanisms for the development of surface charge and recalcitrance in plant-derived biochars. *Environ. Sci. Technol.* **2012**, *46*, 10641–10650.
32. Jiang, X.; Narron, R.H.; Han, Q.; Park, S.; Chang, H.M.; Jameel, H. Tracing Sweetgum Lignin's Molecular Properties through Biorefinery Processing. *ChemSusChem* **2020**, *13*, 4613–4623.
33. He, C.; Giannis, A.; Wang, J.Y. Conversion of sewage sludge to clean solid fuel using hydrothermal carbonization: Hydrochar fuel characteristics and combustion behavior. *Appl. Energy* **2013**, *111*, 257–266.
34. Sonibare, O.O.; Haeger, T.; Foley, S.F. Structural characterization of Nigerian coals by X-ray diffraction, Raman and FTIR spectroscopy. *Energy* **2010**, *35*, 5347–5353.
35. Miliotti, E.; Bettucci, L.; Lotti, G.; Dell'Orco, S.; Rizzo, A.M.; Chiaramonti, D. Hydrothermal carbonization and activation of lignin-rich ethanol co-product. In Proceedings of the 26th European Biomass Conference and Exhibition, Copenhagen, Denmark, 14–18 May 2018.

Disclaimer/Publisher's Note: The statements, opinions and data contained in all publications are solely those of the individual author(s) and contributor(s) and not of MDPI and/or the editor(s). MDPI and/or the editor(s) disclaim responsibility for any injury to people or property resulting from any ideas, methods, instructions or products referred to in the content.